

This paper is published as part of a *CrystEngComm* themed issue entitled:

## Dynamic behaviour and reactivity in crystalline solids

Guest Editors: Tomislav Friščić and Graeme Day  
University of Cambridge, UK

Published in [issue 13, 2011](#) of *CrystEngComm*

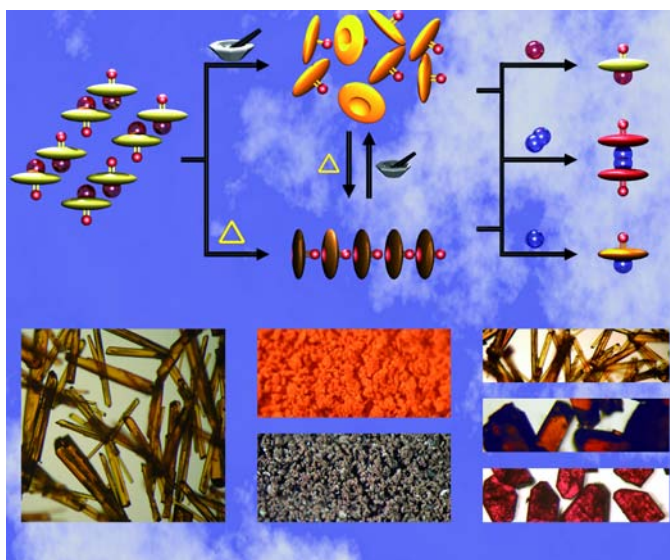


Image reproduced with permission of K. Užarević

Read an editorial article by Sir John Meurig Thomas, University of Cambridge:

[Crystal engineering: origins, early adventures and some current trends](#)

John Meurig Thomas

*CrystEngComm*, 2011, DOI: 10.1039/C1CE90016A

Other articles published in this issue include:

[Drug-drug co-crystals: Temperature-dependent proton mobility in the molecular complex of isoniazid with 4-aminosalicylic acid](#)

Pawel Grobelny, Arijit Mukherjee and Gautam R. Desiraju

*CrystEngComm*, 2011, DOI: 10.1039/C0CE00842G

[Are glycine cyclic dimers stable in aqueous solution?](#)

Said Hamad and C. Richard A. Catlow

*CrystEngComm*, 2011, DOI: 10.1039/C0CE00877J

[Solid-state synthesis of mixed trihalides via reversible absorption of dihalogens by non porous onium salts](#)

L. Meazza, J. Martí-Rujas, G. Terraneo, C. Castiglioni, A. Milani, T. Pilati, Pierangelo Metrangolo and Giuseppe Resnati

*CrystEngComm*, 2011, DOI: 10.1039/C1CE05050H

Visit the *CrystEngComm* website for more cutting-edge crystal engineering research

[www.rsc.org/crystengcomm](http://www.rsc.org/crystengcomm)

Cite this: *CrystEngComm*, 2011, **13**, 4314

www.rsc.org/crystengcomm

PAPER

## Mechanosensitive metal–ligand bonds in the design of new coordination compounds †‡

Krunoslav Užarević,\* Mirta Rubčić,\* Maja Radić, Andreas Puškarić and Marina Cindrić

Received 2nd November 2010, Accepted 22nd December 2010

DOI: 10.1039/c0ce00807a

This article describes the selective cleavage of coordination bonds by mechanochemical methods and the further application of the thus obtained precursors for a facile preparation of new coordination compounds. In the class of dioxomolybdenum(vi) coordination compounds,  $[\text{MoO}_2\text{L}(\text{ROH})]$ , where L stands for a tridentate dianionic ONO ligand and ROH represents different alcohol molecules, mechanical treatment induces an exclusive cleavage of the molybdenum–alcohol bond, which can thus be considered as a mechanosensitive bond. Alcohol removal can also be accomplished by heating. Both grinding and heating resulted in highly reactive, coordinatively unsaturated compounds, an orange amorphous pentacoordinated  $[\text{MoO}_2\text{L}]$  (**I**) and the brown polymeric  $[\text{MoO}_2\text{L}]_n$  (**(I)<sub>n</sub>**), respectively. Even though both **I** and **(I)<sub>n</sub>** are stable at room temperature, they can be interconverted using only solvent-free techniques, a conversion followed by a colour change of the sample. The tendency of such unsaturated complexes to complete their coordination spheres was exploited for the efficient solution and solvent-free syntheses of octahedral molybdenum complexes with selected O- and N-donating ligands. Both approaches herein used, solution and solvent-free, have proved to be superior under specific conditions and their respective advantages and weaknesses are discussed.

### Introduction

In the last few decades, transition metal complexes have been recognized as functional materials with multiple potential applications in *e.g.* host–guest chemistry, catalysis and storage, but also in the design of various electronic and optical devices.<sup>1–3</sup> Such vigorous activity stimulated the development of new and more efficient synthetic routes to various discrete complexes or extended coordination systems. Among the different synthetic approaches, solvent-free methods (grinding, milling, thermal methods, *etc.*) have recently been established as environmentally friendly and, in some aspects, even more efficient alternatives to conventional solution techniques.<sup>4–8</sup> It has been shown that the formation of specific crystal architecture can be controlled by catalytic amounts of solvent<sup>9</sup> or a template.<sup>10</sup> In some cases, the

solvent-free methods also provide a unique route to otherwise inaccessible materials.<sup>11</sup>

In the design of both discrete and extended coordination systems, their synthesis from preorganised homoleptic or heteroleptic coordination compounds is often utilised. Although each of the types is valuable under specific synthetic requirements, heteroleptic complexes tend to be more advantageous when only a certain amount and type of ligands need to be replaced (ancillary). Such an approach also allows a high level of control over the resulting structure because substitution takes place only at strictly defined coordination sites. Furthermore, when the precursor complex contains neutral, volatile ligands, it is sometimes possible to remove that ligand by heating<sup>12</sup> or mechanical<sup>13</sup> treatment, thus producing a coordinatively unsaturated compound. In this context, the solvent-free approaches are more beneficial than the corresponding solution procedures because the coordination of solvent molecules at vacated coordination sites is prevented. The coordinatively unsaturated complexes, due to their higher reactivity, can be considered as “activated” species and, as such, are better precursors, since there is no competition (discrimination) between the departing and the incoming ligand.

Herein, we present a combination and comparison of two approaches, solution and solvent-free, for the efficient synthesis of the octahedral dioxomolybdenum(vi) complexes,  $[\text{MoO}_2\text{L}(\text{D})]$ , where  $\text{H}_2\text{L}$  represents *N*-3-methoxysalicylidene-2-amino-3-hydroxypyridine and D represents the O- (methanol, ethanol, propanol) or N- ( $\gamma$ -picoline, imidazole, 4,4'-bipyridine)

Department of Chemistry, Faculty of Science, University of Zagreb, Horvatovac 102a, 10000 Zagreb, Croatia. E-mail: kruno@chem.pmf.hr; mirta@chem.pmf.hr

† This study is dedicated to the loving memory of Miss Marijana Barišić, dear colleague and friend.

‡ Electronic supplementary information (ESI) available: Detailed syntheses for all obtained products. Thermogravimetric and infrared spectra analyses for all starting compounds and obtained complexes. DSC curves for irreversible transformation of **I** to **(I)<sub>n</sub>**. Selected geometrical parameters and intermolecular C–H...O interactions for all crystallographically investigated compounds and their packing diagrams. Powder patterns for selected products and their comparison. CCDC reference numbers 799774–799781. See DOI: 10.1039/c0ce00807a

donating ligand. The first part of the here presented synthetic path corresponds to the reaction of  $H_2L$  and  $MoO_2(C_3H_7O_2)_2$  in an appropriate alcohol, yielding  $[MoO_2L(ROH)]$  ( $ROH = MeOH: I(Me)$ ,  $EtOH: I(Et)$  and  $PrOH: I(Pr)$ ). The molybdenum–alcohol bonds in such complexes proved to be sensitive to mechanical treatment, *i.e.* they were mechanosensitive, which was further utilised for synthetic purposes. Thus, when such complexes were subjected either to mechanochemical or to thermal treatment, it resulted in the removal of the alcohol ligand, leaving the coordinatively unsaturated pentacoordinated or polymeric complexes,  $[MoO_2L]$  and  $[MoO_2L]_n$ , respectively. It is noteworthy that these “activated” complexes were not attainable by conventional solution synthesis. Both kinds of “activated” complexes were subsequently utilised as highly efficient and reactive precursors in the synthesis of the  $[MoO_2L(D)]$  complexes ( $D$  is the O- or N-donor molecule) *via* various solvent-free routes (vapour sorption, neat grinding and liquid assisted grinding, LAG) and also by conventional solution techniques. All obtained products, as well as their (inter)conversion conditions, were thoroughly characterised by several solid-state methods.

## Results and discussion

The complete synthetic procedure presented here consisted of three steps (Scheme 1): (a) the synthesis of the alcoholic complexes,  $[MoO_2L(ROH)]$ ,  $I(Me)$  ( $ROH = MeOH$ ),  $I(Et)$  ( $ROH = EtOH$ ) and  $I(Pr)$  ( $ROH = PrOH$ ); b) the conversion of the alcoholic complexes to  $[MoO_2L]$  ( $I$ ) or  $[MoO_2L]_n$  ( $I_n$ ) by

mechanochemical or thermal manipulation and c) the preparation of the  $[MoO_2L(D)]$  compounds ( $D$  is the O- or N-donor molecule) from  $I$  or ( $I_n$ ) precursors, *via* both the conventional solution approach and solvent-free routes (vapour sorption, neat grinding and liquid assisted grinding, LAG). When  $D$  was an N-donor, the following  $[MoO_2L(D)]$  products were obtained:  $I(Im)$  and  $I(Im) \cdot CH_3CN$  ( $D = imidazole$ ),  $I(Gp)$  ( $D = \gamma$ -picoline),  $I(Bp)$  and  $I(Bpy) \cdot CH_2Cl_2$  ( $D = 4,4'$ -bipyridine).

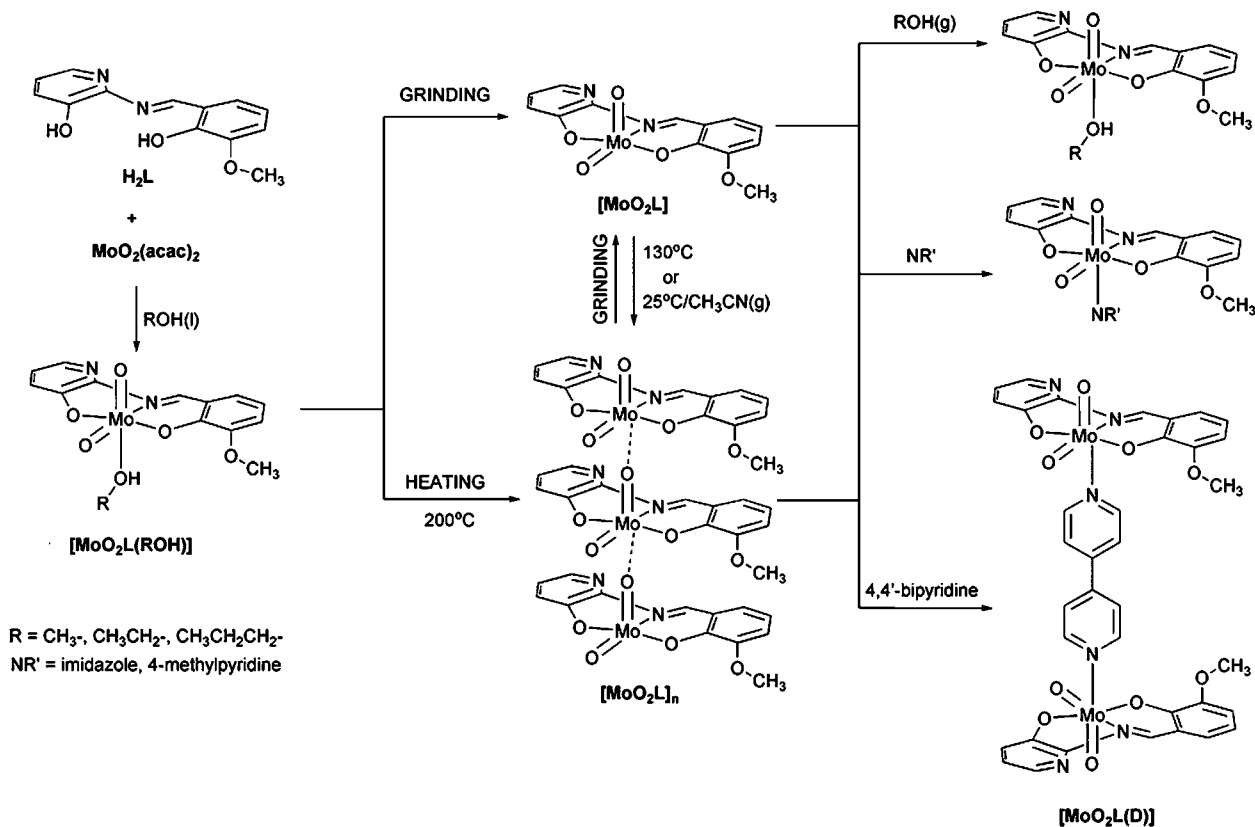
## Experimental

### Materials

Acetylacetone, 3-methoxysalicylaldehyde, 2-amino-3-hydroxypyridine and  $(NH_4)_6Mo_7O_{24} \cdot 4H_2O$  were obtained from Sigma-Aldrich and used without further purification.  $[MoO_2(acac)_2]$ , *cis*-dioxobis(2,4-pentanedionato)molybdenum(vi), was prepared according to the literature methods.<sup>14</sup> The solvents and concentrated acids (p.a. grade) were purchased from Kemika, Zagreb.

### *N*-3-methoxysalicylidene-2-amino-3-hydroxypyridine, $H_2L$

Equimolar amounts (0.82 mmol) of 2-amino-3-hydroxypyridine and 2-hydroxy-3-methoxybenzaldehyde were added to 5 mL of methanol and the mixture was refluxed for 1.5 h. A dark red crystalline product was isolated after 2 d standing at room temperature. Yield: 51%. Elemental analysis calcd (found) for  $C_{13}H_{12}N_2O_3$ : C 63.93 (63.97), H 4.95 (4.88), N 11.47 (11.40). IR



**Scheme 1** Summary of the synthetic pathways and interconversion conditions for the investigated  $[MoO_2L(D)]$  coordination compounds and  $[MoO_2L]/[MoO_2L]_n$  system.

(KBr,  $\text{cm}^{-1}$ ): 3428 br ( $\nu_{\text{O-H}}$ ), 3050, 3006 br ( $\nu_{\text{C-H}}$ ), 1617, 1577, 1544, 1520 ( $\nu_{\text{C=O}}$  and  $\nu_{\text{C=N}}$ ).

### Syntheses of alcohol complexes

**(A) General solution procedure.**  $[\text{MoO}_2(\text{acac})_2]$  (94 mg, 0.29 mmol) was added to a solution (5 mL) of  $\text{H}_2\text{L}$  (70 mg, 0.29 mmol) in 5 mL of the corresponding alcohol and refluxed for 1.5 h. After 1 d (ethanol and propanol) or 3 d (methanol) standing at room temperature, stable orange crystals were isolated, washed with small amount of solvent and collected. Crystals appropriate for the diffraction experiments were collected from  $3\times$  diluted reaction mixtures and on prolonged standing.

**$[\text{MoO}_2\text{L}(\text{MeOH})]$ , **I(Me)**.** Yield: 77%. Elemental analysis calcd (found) for  $\text{C}_{14}\text{H}_{14}\text{N}_2\text{O}_6\text{Mo}$ : C 41.81 (41.92), H 3.51 (3.50), N 6.96 (7.05). IR (KBr,  $\text{cm}^{-1}$ ): 3469 br ( $\nu_{\text{O-H}}$ ), 2562 ( $\nu_{\text{C-H}}$ ), 1605, 1584, 1553 ( $\nu_{\text{C=O}}$  and  $\nu_{\text{C=N}}$ ), 1014 ( $\nu_{\text{C-O}}$ , methanol), 938, 914 ( $\nu_{\text{Mo=O}}$ , terminal).

**$[\text{MoO}_2\text{L}(\text{EtOH})]$ , **I(Et)**.** Yield: 66%. Elemental analysis calcd (found) for  $\text{C}_{15}\text{H}_{16}\text{N}_2\text{O}_6\text{Mo}$ : C 43.28 (43.20), H 3.87 (3.74), N 6.73 (6.90). IR (KBr,  $\text{cm}^{-1}$ ): 3447 br ( $\nu_{\text{O-H}}$ ), 2821 ( $\nu_{\text{C-H}}$ ), 1605, 1581, 1553 ( $\nu_{\text{C=O}}$  and  $\nu_{\text{C=N}}$ ), 1035 ( $\nu_{\text{C-O}}$ , ethanol), 933, 911 ( $\nu_{\text{Mo=O}}$ , terminal).

**$[\text{MoO}_2\text{L}(\text{PrOH})]$ , **I(Pr)**.** Yield: 89%. Elemental analysis calcd (found) for  $\text{C}_{16}\text{H}_{18}\text{N}_2\text{O}_6\text{Mo}$ : C 44.66 (44.71), H 4.22 (4.17), N 6.51 (6.50). IR (KBr,  $\text{cm}^{-1}$ ): 3419 br ( $\nu_{\text{O-H}}$ ), 2957, 2835 ( $\nu_{\text{C-H}}$ ), 1598, 1581, 1553 ( $\nu_{\text{C=O}}$  and  $\nu_{\text{C=N}}$ ), 1039 ( $\nu_{\text{C-O}}$ , propanol), 936, 913 ( $\nu_{\text{Mo=O}}$ , terminal).

**(B) Vapour sorption experiments.** **I** or **(I)<sub>n</sub>** (0.04 mmol) was placed in the sealed beaker with alcohol vapours. The orange or brown precursor changed colour after 10 min (methanol) or 1 d (ethanol and propanol) standing at room temperature. Analyses (elemental analysis, PXRD, IR) of the product show that the synthesised yellow crystals correspond to a  $[\text{MoO}_2\text{L}(\text{ROH})]$  coordination compound. Yield: 100%.

### Syntheses of coordinatively unsaturated complexes, $[\text{MoO}_2\text{L}]$ and $[\text{MoO}_2\text{L}]_n$

**$[\text{MoO}_2\text{L}]$ , **I**.** All three alcohol complexes, **I(Me)**, **I(Et)** or **I(Pr)** were ground using a mortar and a pestle for 5 min. Depending on the complex being ground, a different time of grinding was needed for the yellow powders to change colour to dark orange (5 min for **I(Me)**, 15 min for **I(Et)** and 35 min for **I(Pr)**). The process was repeated under an inert atmosphere (argon) with the same result. The amorphous (PXRD) substance thus prepared, **I**, was collected and analysed. Elemental analysis calcd (found) for  $\text{C}_{13}\text{H}_{10}\text{N}_2\text{O}_5\text{Mo}$ : C 42.18 (42.02), H 2.72 (2.56), N 7.57 (7.63). IR (KBr,  $\text{cm}^{-1}$ ): 2936, 2836 ( $\nu_{\text{C-H}}$ ) 1598, 1553 ( $\nu_{\text{C=O}}$  and  $\nu_{\text{C=N}}$ ), 939, 911 ( $\nu_{\text{Mo=O}}$ , terminal).

#### $[\text{MoO}_2\text{L}]_m$ , **(I)<sub>n</sub>**

**Method I. Heating of alcohol complexes.** Synthesis of **(I)<sub>n</sub>** was conducted using a simple furnace or a thermogravimetric

balance. The alcohol complexes were placed in a crucible and heated to 210 °C, at 5 °C  $\text{min}^{-1}$ . In all cases, this procedure resulted in a brown product, **(I)<sub>n</sub>** in quantitative yield. Elemental analysis calcd (found) for  $\text{C}_{13}\text{H}_{10}\text{N}_2\text{O}_5\text{Mo}$ : C 42.18 (42.06), H 2.72 (2.80), N 7.57 (7.55). IR (KBr,  $\text{cm}^{-1}$ ): 2925, 2834 ( $\nu_{\text{C-H}}$ ), 1606, 1594, 1551 ( $\nu_{\text{C=O}}$  and  $\nu_{\text{C=N}}$ ), 941 ( $\nu_{\text{Mo=O}}$ , terminal), 814 s, br ( $\nu_{\text{Mo=O}\cdots\text{Mo}}$ ).

**Method II.** **I** was heated from 25 °C to 130 °C (5 °C  $\text{min}^{-1}$ ) and cooled to room temperature. Analytical and spectral data for the isolated product obtained by this method are in agreement with those of the compound prepared according to method *I*.

### Syntheses of $[\text{MoO}_2\text{L}(\text{D})]$ complexes with N-donors

**(C) Solution syntheses from dichloromethane or acetonitrile.**  $[\text{MoO}_2\text{L}]$  or  $[\text{MoO}_2\text{L}]_n$  (15 mg, 0.04 mmol) were diluted in 1.5 mL of heated dry solvent. To such a prepared solution, an equimolar amount of the N-donor was added and the reaction mixture was refluxed for 20 min. Products were filtered off and dried after 2 d standing at room temperature. Depending on the solvent used, different solvated or unsolvated materials were obtained.

**$[\text{MoO}_2\text{L}(\text{im})]$ , **I(Im)**.** Solvent used: dichloromethane; orange needles. Yield: 66%. Elemental analysis calcd (found) for  $\text{C}_{16}\text{H}_{14}\text{N}_4\text{O}_5\text{Mo}$ : C 43.85 (43.76), H 3.22 (3.16), N 12.78 (12.64). IR (KBr,  $\text{cm}^{-1}$ ): 3284m ( $\nu_{\text{N-H}}$ , imidazole), 2944, 2837 ( $\nu_{\text{C-H}}$ ), 1603, 1553 ( $\nu_{\text{C=O}}$  and  $\nu_{\text{C=N}}$ ), 927 s, 902, 896 ( $\nu_{\text{Mo=O}}$ , terminal).

**$[\text{MoO}_2\text{L}(\text{im})]\cdot\text{CH}_3\text{CN}$ , **I(Im)\cdot\text{CH}\_3\text{CN}**.** Solvent used: acetonitrile; red prisms. Yield: 47%. Elemental analysis calcd (found) for  $\text{C}_{17}\text{H}_{15}\text{N}_5\text{O}_5\text{Mo}$ : C 43.88 (43.82), H 3.25 (3.22), N 15.05 (15.11). IR (KBr,  $\text{cm}^{-1}$ ): 3327m ( $\nu_{\text{N-H}}$  imidazole), 2950, 2843 ( $\nu_{\text{C-H}}$ ), 2248 ( $\nu_{\text{C}\equiv\text{N}}$  acetonitrile), 1600, 1553 ( $\nu_{\text{C=O}}$  and  $\nu_{\text{C=N}}$ ), 924s, 902s ( $\nu_{\text{Mo=O}}$ , terminal).

**$[\text{MoO}_2\text{L}(\gamma\text{-pic})]\cdot\text{CH}_3\text{CN}$ , **I(Gp)\cdot\text{CH}\_3\text{CN}**.** Solvent used: acetonitrile; red prisms. Yield: 69%. Elemental analysis calcd (found) for  $\text{C}_{20}\text{H}_{18}\text{N}_4\text{O}_5\text{Mo}$ : C 48.99 (48.97), H 3.70 (3.66), N 11.43 (11.40). IR (KBr,  $\text{cm}^{-1}$ ): 2995m, 2832m ( $\nu_{\text{C-H}}$ ), 2251 ( $\nu_{\text{C}\equiv\text{N}}$  acetonitrile), 1618, 1598, 1551 ( $\nu_{\text{C=O}}$  and  $\nu_{\text{C=N}}$ ), 925s, 903s ( $\nu_{\text{Mo=O}}$ , terminal), 740 ( $\nu_{\text{Mo-O}}$  and  $\nu_{\text{Mo-N}}$ ).

**$(\text{MoO}_2\text{L})_2(\text{bpy})\cdot\text{CH}_2\text{Cl}_2$ , **I(Bp)\cdot\text{CH}\_2\text{Cl}\_2**.** Solvent used: dichloromethane; red prisms. Elemental analysis calcd (found) for  $\text{C}_{37}\text{H}_{30}\text{N}_6\text{O}_{10}\text{Mo}_2\text{Cl}_2$ : C 45.28 (45.26), H 3.08 (3.10), N 8.56 (8.62). IR (KBr,  $\text{cm}^{-1}$ ): 3043-2849 ( $\nu_{\text{C-H}}$ ), 1605, 1596, 1553 ( $\nu_{\text{C=O}}$  and  $\nu_{\text{C=N}}$ ), 927s, 905 ( $\nu_{\text{Mo=O}}$ , terminal), 749, 729 ( $\nu_{\text{Mo-O}}$  and  $\nu_{\text{Mo-N}}$ ).

**$(\text{MoO}_2\text{L})_2(\text{bpy})$ , **I(Bp)**.** Solvent used: acetonitrile; red prisms. Elemental analysis calcd (found) for  $\text{C}_{36}\text{H}_{28}\text{N}_6\text{O}_{10}\text{Mo}_2$ : C 48.23 (48.26), H 3.15 (3.11), N 9.37 (9.42). IR (KBr,  $\text{cm}^{-1}$ ): 3051-2830 ( $\nu_{\text{C-H}}$ ), 1598, 1550 ( $\nu_{\text{C=O}}$  and  $\nu_{\text{C=N}}$ ), 928s, 906 ( $\nu_{\text{Mo=O}}$ , terminal), 744, 733 ( $\nu_{\text{Mo-O}}$  and  $\nu_{\text{Mo-N}}$ ).

**(D) Liquid assisted grinding of **I** or **(I)<sub>n</sub>** in the presence of appropriate N-donor.** **I** or **(I)<sub>n</sub>** (15 mg, 0.04 mmol) and an equimolar amount of the N-donor (1 : 1 with imidazole or  $\gamma$ -picoline,

1 : 0.5 with bipyridine) were placed in the 5 mL steel jar (1 steel ball). From two to four drops of acetonitrile or dichloromethane were added. The jar was sealed and placed in the Retsch MM 200 ball mill (25 Hz, 25 min). The collected orange microcrystalline products were analysed by usual methods (IR, PXRD) and it was established that some ground products were the same as those obtained by classic solution methods, but with improved yields (quantitative). However, this method was unsuccessful for the synthesis of the alcohol complexes, **I(Im)·CH<sub>3</sub>CN** and **I(Bp)·CH<sub>2</sub>Cl<sub>2</sub>**. In the case of the alcohol complexes, **I** was obtained. In the case of the above-mentioned two solvated N-complexes, the N-ligand successfully coordinated on the sixth place, but no solvent molecules were present in the structure.

**(E) Neat grinding of I or (I)<sub>n</sub> in the presence of appropriate N-donor.** **I** or **(I)<sub>n</sub>** (15 mg, 0.04 mmol) and an equimolar amount of the N-donor were placed in the 5 mL steel jar (1 steel ball). The jar was placed in the Retsch MM 200 ball mill (25 Hz, 25 min). The collected orange amorphous products were analysed by IR and PXRD. There were no traces of starting compounds in the PXRD patterns and also the IR spectra were identical to the products obtained by LAG or solution synthesis. However, to gain crystalline products, LAG and solution synthetic approaches were preferred.

**Methods.** Elemental analyses were performed by Central Analytical Service, “Ruder Bošković” Institute, Zagreb. IR spectra were recorded on a PerkinElmer Spectrum RXI FT-IR spectrometer (KBr pellet technique, 4000–400 cm<sup>-1</sup> range, 2 cm<sup>-1</sup> step). Temperature-resolved IR were collected on a Bruker VECTOR 22 FT-IR spectrometer (KBr pellet technique, 4000–400 cm<sup>-1</sup> range, 2 cm<sup>-1</sup> step) in the range from 25 to 180 °C. Thermogravimetric analyses (TGA) were performed on a Mettler-Toledo TGA/SDTA851° thermobalance using aluminium crucibles under a nitrogen or oxygen stream with the heating rate of 5 °C min<sup>-1</sup>. In all experiments the temperature range was from 25 to 600 °C. The results were processed with the Mettler STARE 9.01 software. DSC measurements were performed on the Mettler-Toledo DSC823° calorimeter with STARE SW 9.01 in the range from 25 to maximally 600 °C (5 °C min<sup>-1</sup>) under the nitrogen stream.

**X-Ray diffraction experiments.** Selected crystallographic and refinement data for the reported structures were obtained by single-crystal X-ray diffraction experiments and are reported in Table 1. The data for all structures were collected by  $\omega$ -scans on an Oxford Xcalibur diffractometer equipped with 4-circle kappa geometry and a CCD Sapphire 3 detector and graphite-monochromated Mo-K $\alpha$  radiation at 295 K. The programs CrysAlis CCD and CrysAlis RED<sup>15</sup> were employed for data collection, cell refinement and data reduction. Structures were solved by direct methods and refined on  $F^2$  by weighted full-matrix least-squares. The programs SHELXS-97<sup>16</sup> and SHELXL-97,<sup>17</sup> integrated in the WinGX software system,<sup>18</sup> were used to solve and refine the structures. All non-hydrogen atoms were refined anisotropically, while the restraints on geometrical and displacement parameters (DFIX, SAME, DELU, SIMU and EADP) were applied for the disordered ethanol and propanol residues in **I(Et)** and **I(Pr)**. Hydrogen atoms attached to carbon atoms were placed in

geometrically idealized positions and refined applying the riding model. Hydrogen atoms belonging to the coordinated alcohol moieties (H6O in **I(Me)**, **I(Et)** and **I(Pr)**) and imidazole molecules (H4N in **I(Im)·CH<sub>3</sub>CN** and **I(Im)**) were located in the difference Fourier maps at the final stages of refinement procedure and their coordinates were refined freely but with the restrained O–H/N–H distance of 0.82 Å/0.86 Å. The geometrical calculations and structural analyses were done using PLATON,<sup>19</sup> while graphics were done with ORTEP,<sup>20</sup> POV-Ray<sup>21</sup> and Mercury.<sup>22</sup> Selected bond lengths and valence angles are listed in Table S1.†

X-Ray powder diffraction experiments were performed on a Philips PW 3710 diffractometer using Cu-K $\alpha$  radiation, with a zero background sample holder in the Bragg-Brentano geometry; tension 40 kV, current 40 mA. The patterns were collected in the angle region between 4° and 40° (2 $\theta$ ) with a step size of 0.02° and 1.0 s counting per step.

### Crystallographic studies

The crystallographic data for all investigated compounds are given in Table 1. The molecular structures for compounds **I(Me)** and **I(Im)**, as examples of the [MoO<sub>2</sub>L(ROH)] and [MoO<sub>2</sub>L(N-donor)] complexes, are presented in Fig. 1. The molecular structures for compounds **I(Et)**, **I(Pr)**, **I(Im)·CH<sub>3</sub>CN**, **I(Gp)**, **I(Bp)** and **I(Bp)·CH<sub>2</sub>Cl<sub>2</sub>** and their atom labelling schemes are shown in Fig. S2–S4.‡ In all structures the atoms of the coordinated ligand (L<sup>2-</sup>) are labelled in the same way.

The main building unit for all the mononuclear and dinuclear complexes is the MoO<sub>2</sub><sup>2+</sup> core with *cis*-arranged oxo moieties. In each complex the core is accommodated in such a way that the molybdenum(vi) ion becomes a centre of a distorted octahedron, while the tridentate ONO ligand binds in an equatorial position. Relevant bond distances support the fact that the ligand is coordinated in a dianionic (L<sup>2-</sup>) manner with the system of conjugated bonds spreading along the two chelate rings (Tables S1–S4.†). Finally, the coordination sphere is filled with the corresponding O- or N-donor molecule (alcohol or N-base) at the sixth coordination site. With alcohols, imidazole or  $\gamma$ -picoline as the ancillary ligands mononuclear complexes are obtained, while dinuclear compounds form with the bridging 4,4'-bipyridine. The *trans* effect of the oxygen atoms of the MoO<sub>2</sub><sup>2+</sup> unit is manifested through the elongated Mo(1)–N(2), where the N(2) atom belongs to the L<sup>2-</sup> ligand and the Mo–O/N(ancillary ligand) bonds (Tables S1–S4.†).

The conformational differences between similar complexes are evident in the various degrees of planarity of the coordinated ligand, *i.e.* the relative position of the phenyl and pyridyl rings (Fig. 2). Additionally, the diverse spatial arrangements of the monodentately bound O or N ligands (alcohol or N-base) induce further conformational differences, which is particularly obvious for the two imidazole complexes and the two bipyridine complexes (Fig. 2).

The packing interactions and, consequently, the crystal structures of the investigated compounds differ considerably with respect to (a) the presence of hydrogen bond donors at the auxiliary ligands bound at the sixth coordination site and (b) the presence of the solvent molecules within the crystal lattice. If a hydrogen bond donor is present within the ancillary ligand, two

**Table 1** Crystallographic data for **I(Me)**, **I(Et)**, **I(Pr)**, **I(Im)**, **I(CH<sub>3</sub>CN)**, **I(Gp)·CH<sub>3</sub>CN**, **I(Bp)** and **I(Bp)·CH<sub>2</sub>Cl<sub>2</sub>**.<sup>a</sup>

	<b>I(Me)</b>	<b>I(Et)</b>	<b>I(Pr)</b>	<b>I(Gp)·CH<sub>3</sub>CN</b>	<b>I(Im)·CH<sub>3</sub>CN</b>	<b>I(Bp)</b>	<b>I(Bp)·CH<sub>2</sub>Cl<sub>2</sub></b>
Empirical formula	C <sub>14</sub> H <sub>14</sub> N <sub>2</sub> O <sub>6</sub> Mo	C <sub>13</sub> H <sub>16</sub> N <sub>2</sub> O <sub>6</sub> Mo	C <sub>16</sub> H <sub>18</sub> N <sub>2</sub> O <sub>6</sub> Mo	C <sub>19</sub> H <sub>17</sub> N <sub>3</sub> O <sub>5</sub> Mo· C <sub>2</sub> H <sub>3</sub> N	C <sub>16</sub> H <sub>14</sub> N <sub>4</sub> O <sub>5</sub> Mo· C <sub>2</sub> H <sub>3</sub> N	C <sub>36</sub> H <sub>28</sub> N <sub>6</sub> O <sub>10</sub> Mo <sub>2</sub>	C <sub>36</sub> H <sub>28</sub> N <sub>6</sub> O <sub>10</sub> Mo <sub>2</sub> · 2(CH <sub>2</sub> Cl <sub>2</sub> )
Formula weight/ g mol <sup>-1</sup>	402.21	416.24	430.26	504.35	479.31	896.52	1066.38
Crystal system	Monoclinic	Monoclinic	Triclinic	Monoclinic	Monoclinic	Triclinic	Monoclinic
Crystal size/mm	0.40 × 0.25 × 0.08	0.30 × 0.10 × 0.05	0.35 × 0.15 × 0.12	0.08 × 0.06 × 0.04	0.34 × 0.08 × 0.05	0.40 × 0.10 × 0.10	0.10 × 0.06 × 0.03
Crystal habit	Prism	Prism	Prism	Prism	Prism	Prism	Prism
Crystal color	Orange	Orange	Orange	Red	Orange	Red	Red
Space group	<i>P</i> 2 <sub>1</sub> / <i>c</i>	<i>P</i> 2 <sub>1</sub> / <i>c</i>	<i>P</i> 1	<i>P</i> 2 <sub>1</sub> / <i>c</i>	<i>P</i> 2 <sub>1</sub> / <i>c</i>	<i>P</i> 1	<i>P</i> 2 <sub>1</sub> / <i>c</i>
Unit cell dimensions							
<i>a</i> /Å	8.1890(7)	8.0992(16)	7.7894(4)	8.8879(3)	7.5668(3)	11.7871(6)	12.342(1)
<i>b</i> /Å	10.9898(9)	11.404(1)	10.0907(7)	14.5134(5)	19.3973(7)	12.8269(7)	13.4804(9)
<i>c</i> /Å	17.930(2)	17.993(3)	12.5937(5)	16.4716(6)	14.5305(6)	13.8071(6)	17.344(2)
<i>α</i> /°	90	90	86.293(4)	90	90	108.490(5)	90
<i>β</i> /°	105.346(9)	99.47(2)	81.553(4)	90.433(3)	116.626(3)	94.104(4)	131.638(6)
<i>γ</i> /°	90	90	69.096(5)	90	90	113.811(5)	90
Volume/Å <sup>3</sup>	1556.1(3)	1639.2(4)	914.61(9)	2124.7(1)	1906.6(1)	1762.7(2)	2156.5(3)
<i>Z</i>	4	4	2	4	4	2	2
<i>D</i> <sub>c</sub> /g cm <sup>-3</sup>	1.717	1.687	1.562	1.577	1.670	1.689	1.642
<i>μ</i> /mm <sup>-1</sup>	0.875	0.834	0.750	0.658	0.730	0.780	0.891
<i>F</i> (000)	808	840	436	1024	968	900	1068
Reflections collected/ unique	6270/3210	11 592/3549	6752/3761	9891/4400	7292/3536	18 949/9792	8185/4446
Data/restraints/ parameters	3210/1/212	3549/18/218	3761/60/218	4400/0/281	3536/1/266	9792/0/487	4446/0/272
<i>S</i> /Restrained <i>S</i>	0.923/0.923	1.018/1.015	0.982/0.975	1.050/1.050	1.023/1.024	0.940/0.940	0.940/0.940
<i>R</i> / <i>wR</i> <sub>2</sub> [ <i>I</i> > 2σ( <i>I</i> )] <sup>a</sup>	0.0240/0.0616	0.0331/0.0777	0.0461/0.1259	0.0361/0.0670	0.0333/0.0615	0.0396/0.1045	0.0348/0.0933
Largest diff. peak, hole/e Å <sup>-3</sup>	0.282, -0.562	0.388, -0.423	1.602, -1.391	0.376, -0.359	0.269, -0.296	0.957, -0.538	0.633, -0.684

<sup>a</sup>  $R = \sum |F_o| - |F_c| / \sum F_o$ ,  $w = 1/[\sigma^2(F_o^2) + (g_1/P)^2 + g_2/P]$  where  $P = (F_o^2 + 2F_c^2)/3$ ,  $wR_2 = \{\sum [w(F_o^2 - F_c^2)^2] / \sum wF_o^2\}^{1/2}$ ,  $S = \{\sum [w(F_o^2 - F_c^2)^2] / (N_{obs} - N_{param})\}^{1/2}$ .

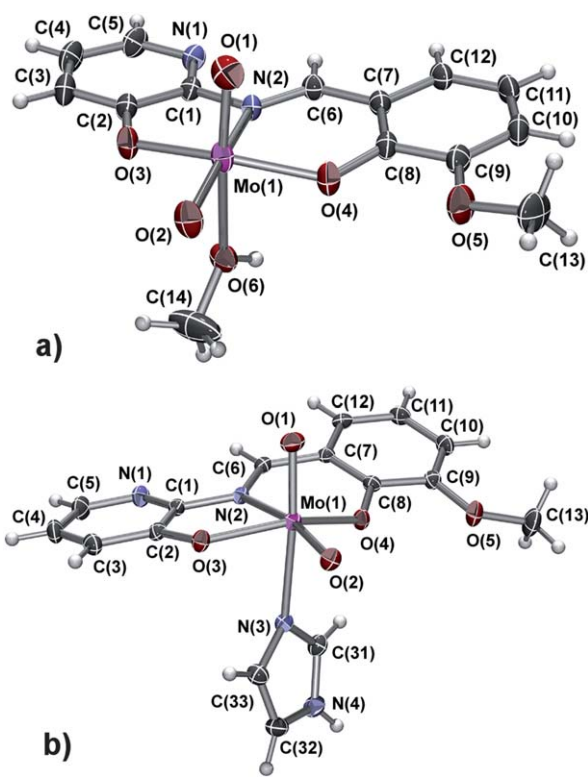


**Fig. 1** ORTEP-POV-Ray rendered view of the molecular structures for (a) **I(Me)** and (b) **I(Im)** with the atom-numbering schemes. Displacement ellipsoids are drawn at the 30% probability level. Hydrogen atoms are presented as spheres of arbitrary small radii.

primary architectures are distinguished: hydrogen bonded dimers and hydrogen bonded chains (Fig. 3).

In the case of the alcoholic complexes, dimers are realized through  $R_2^2(12)$  O(6)–H(6)···N(1) hydrogen bonds (Fig. 3a). Such dimers are further associated *via* C–H···O interactions into a three-dimensional architecture (Fig. S5†). A similar building unit is found in the structure of **I(Im)** but the dimers form through  $R_2^2(12)$  N(4)–H(4N)···O(2) hydrogen bonds (Fig. 3b and Fig. S8†). The same N–H functionality additionally participates in N(4)–H(4N)···O(3) hydrogen bonds, which join dimers, thus forming a bifurcated hydrogen bond [(N(4)–H(4N)) 0.857(15) Å, H(4N)···O(3) 2.386(18) Å, N(4)···O(3) 3.087(2) Å, N(4)–H(4N)···O(3) 139(2)°, (i) = –1+x, y, z]. On the other hand, in the structure of the solvate complex, **I(Im)·CH<sub>3</sub>CN**, another oxygen atom, O(5), is used as the hydrogen bond acceptor. This subsequently prevents the emergence of the dimeric synthon and leads to a considerably different primary architecture, namely the  $C_1^1(9)$  N(4)–H(4N)···O(5) hydrogen bonded chains (Fig. 3c). The acetonitrile molecules bridge such chains *via* C–H···O and C–H···N interactions. In the absence of a good hydrogen bond donor in auxiliary moieties, the stabilization of the structure is achieved through the strongest disposable interactions, namely the C–H···O and C–H···N interactions (Fig. S9†). A rather intricate architecture is found in the **I(Gp)·CH<sub>3</sub>CN**, due to the exceedingly rich interplay of such interactions, which employ both the complex and acetonitrile molecules (Fig. S10†). The crystal structures of the solvatomorphic pair, **I(Bp)** and **I(Bp)·CH<sub>2</sub>Cl<sub>2</sub>**, display significant differences. In the

**I(Bp)·CH<sub>2</sub>Cl<sub>2</sub>**, C–H···O and C–H···N interactions, which include both the complex and the solvent molecules, assemble the molecules into layers (in the *bc* plane), which are further stacked along the *a* axis. In the unsolvated dinuclear product, **I(Bp)**, the molecules are arranged into a complicated three-dimensional architecture, through C–H···O and C–H···N interactions, however without forming a layered architecture (Fig. S11 and Fig. S12†).

### Synthesis and characteristics of [MoO<sub>2</sub>L(ROH)], **I** and **I<sub>n</sub>** complexes

The reactions of MoO<sub>2</sub>(*acac*)<sub>2</sub> and H<sub>2</sub>L in methanol, ethanol or propanol readily produced dioxomolybdenum(vi) complexes of the general formula [MoO<sub>2</sub>L(ROH)], in fairly satisfying yields. In all cases, the ligand coordinates to the MoO<sub>2</sub><sup>2+</sup> core, with oxo moieties in the *cis* arrangement, as a dianionic tridentate ONO donor. The overall coordination geometry of the compounds is octahedral. With the equatorially bound ligand, the neutral ROH moiety is accommodated *trans* to the apical oxygen atom. Due to the strong *trans* influence of the oxo ligands, the bonds on this coordination site tend to be elongated.<sup>23</sup>

As we already noted, it is well known that weakly coordinated ligands are, upon heating, often liberated from coordination compounds.<sup>12</sup> New complexes, thus formed, possess an unsaturated coordination environment and can thus be considered as “activated”. Such complexes can be exploited as starting materials for the further syntheses of coordination compounds, due to their tendency to re-complete the coordination spheres. During our recent study on the polymorphism of a methanolic dioxomolybdenum(vi) complex,<sup>13</sup> we established that the formation of such an “activated” species can be accomplished not only through heating, but also by mechanochemical treatment. Among all the metal–ligand bonds of the coordination sphere of the investigated [MoO<sub>2</sub>L(ROH)] compounds, the Mo–O(alcohol) bonds are the longest and consequently the weakest (Table S1†). Additionally, the alcohol molecules are bound as neutral species in a monodentate fashion, which makes them likely candidates for the selective dissociation of the metal–alcohol coordination bond.

Thermal manipulations were conducted and monitored by a thermogravimetric balance (TG), differential scanning calorimetry (DSC) and temperature-resolved infrared spectroscopy (TR-IR). All investigated alcohol complexes displayed similar behaviour, with the first thermal event occurring in the temperature range between 100 °C and 210 °C. This corresponds to the dissociation of the coordinated alcohol molecule (Fig. 4 and Fig. S1, ESI†) and, for all alcohol complexes, this yielded the same brown microcrystalline product (PXRD, Fig. S13†). The highest temperature for the removal of the alcohol ligand was needed for **I(Me)**. However, we have taken this compound as the model-complex for solid-state transformations due to the following: (a) among all the alcoholic complexes the [MoO<sub>2</sub>L(MeOH)] can be obtained without the need for further purification and in a high yield and (b) methanol was the most readily removed from a solid material in mechanochemical treatments.

The elemental analysis of the brown product confirmed the absence of alcohol ligands, *i.e.* the empirical formula of the product is [MoO<sub>2</sub>L]. The *cis*-dioxomolybdenum complexes have

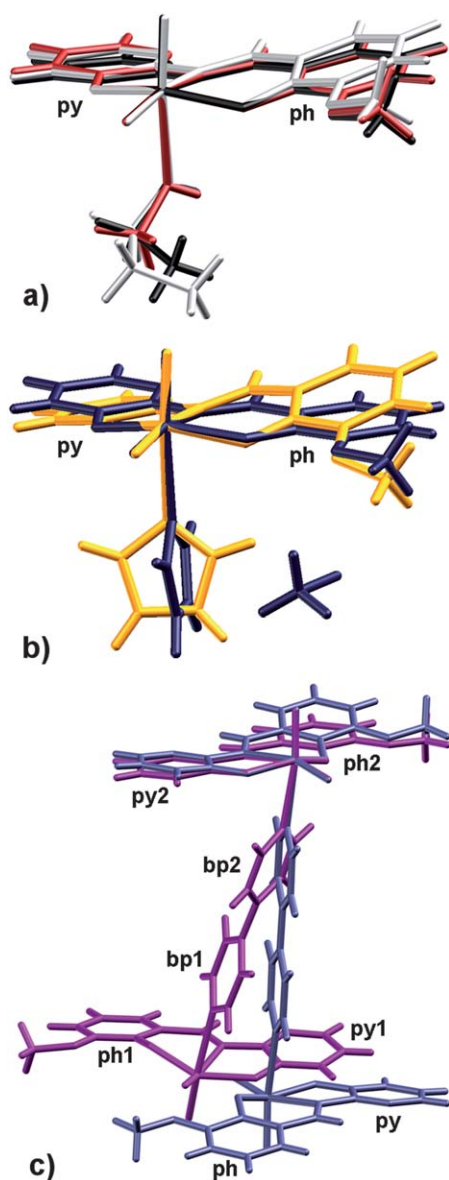


**Fig. 2** Mercury-POV-Ray rendered view of overlapping diagrams for (a) alcohol complexes; **I(Me)** red, **I(Et)** black, **I(Pr)** gray; (b) imidazole complexes; **I(Im)·CH<sub>3</sub>CN** blue, **I(Im)** orange and (c) bipyridine complexes; **I(Bp)·CH<sub>2</sub>Cl<sub>2</sub>** blue, **I(Bp)** purple. Diagrams were constructed by overlapping molecules through Mo(1), O(1), O(2) and O(3) atoms. Dihedral angles between the planes of phenyl (ph) and pyridyl (py) are: (a) 8.3(1)° for **I(Me)**, 12.0(2)° for **I(Et)**, 13.0(2)° **I(Pr)**; (b) 0.9(2)° for **I(Im)·CH<sub>3</sub>CN** and 21.3(1)° for **I(Im)** and (c) 17.0(2)° for **I(Bpy)·CH<sub>2</sub>Cl<sub>2</sub>**. In **I(Bpy)** the two halves of the complex are non-equivalent and the dihedral angles between the planes ph1 and py1 and ph2 and py2 amount to 11.2(2)° and 2.9(2)° respectively. Additionally, the dihedral angles between the two rings of the bridging 4,4'-bipyridine, Bp1 and Bp2, is 44.9(2)°.

a pronounced tendency to form dinuclear or polynuclear complexes in the absence of suitable donor species for the sixth coordination site.<sup>24</sup> In this way, octahedral or at least quasi-octahedral coordination is accomplished, which is favourable compared to the pentacoordinated one. The polymeric structure is realized *via* Mo=O···Mo interactions of the neighbouring

mononuclear units, which is indicated by several characteristic changes in the IR spectra. The vibration of the Mo=O···Mo moiety causes the emergence of a broad band in the range 750–800 cm<sup>-1</sup>. Additionally, the spectra of the compounds with such polymeric structure display only one band characteristic for the terminal Mo=O vibration due to the involvement of the one Mo=O<sub>terminal</sub> group in the Mo=O···Mo interaction. The IR spectrum of the brown product revealed exactly such features: (a) only one strong and visible Mo=O<sub>terminal</sub> vibration band, more precisely the one at 941 cm<sup>-1</sup> and (b) the appearance of a strong and broad band at 814 cm<sup>-1</sup>, due to the vibration of Mo=O···Mo moiety. Thus, it was concluded that the brown product, obtained by heating, has the polymeric structure, [MoO<sub>2</sub>L]<sub>n</sub> (**I<sub>n</sub>**).

In the solid-state approach, all [MoO<sub>2</sub>L(ROH)] compounds were ground at room temperature using a mortar and pestle. Use of a ball mill was avoided, to allow the removal of alcoholic vapours from the system. The samples changed their original colour to dark orange during grinding, which was stable upon prolonged grinding. The analysis (TGA, IR and elemental analysis) of the thus obtained orange product revealed it does not contain coordinated alcohol molecules and has an empirical formula of [MoO<sub>2</sub>L]. In this case as well, IR spectroscopy proved to be a very powerful tool for elucidating the product's structure.

The IR spectra of the orange product revealed the bands characteristic for Mo=O<sub>term</sub> stretching, which were similar to those of the alcohol complexes but with the intensities reduced. These features, along with the absence of the band characteristic for the alcoholic C–O stretching (at 1014 cm<sup>-1</sup> in the [MoO<sub>2</sub>L(ROH)] complexes), correspond to a mononuclear penta-coordinated complex, [MoO<sub>2</sub>L] (**I**).

It is worth mentioning that the usual solution synthetic routes to the polymeric (**I<sub>n</sub>**) or pentacoordinated **I**, by the reaction of H<sub>2</sub>L and MoO<sub>2</sub>(acac)<sub>2</sub> in acetonitrile or dichloromethane, were, in this particular case, unsuccessful. Namely, in each attempt, the water molecules, from the solvent or from the atmosphere, readily coordinated to the sixth coordination place, yielding [MoO<sub>2</sub>L(H<sub>2</sub>O)], even if the reaction and isolation were performed using dry solvents and in an inert (argon) atmosphere.

### Transformations between **I** and (**I<sub>n</sub>**) complexes

To establish the relative stability and possible interconversion conditions between two coordinatively unsaturated precursors, a number of solvent-free experiments were conducted (Fig. 5, Scheme 1). Heating the orange **I** resulted in two consecutive thermal events, *i.e.* a broad endotherm with an onset at ~60 °C followed by an exotherm at 144 °C (Fig. S1, ESI<sup>†</sup>). These thermal events were ascribed to a transformation of the mononuclear **I** to the brown (**I<sub>n</sub>**) (PXR), through the formation of Mo=O···Mo interactions. This conversion was monitored by temperature-resolved IR (TR-IR, heating rate was 5 °C min<sup>-1</sup>), measured on the thin plate of [MoO<sub>2</sub>L]. This method provided valuable dynamic insight on the changes in the molecular structure of **I** during the **I** to (**I<sub>n</sub>**) transformation (Fig. 6). The changes in the coordination sphere of the molybdenum cation are especially visible in the region between 1000 and 600 cm<sup>-1</sup>, as previously discussed. During the transformation process, several bands characteristic for (**I<sub>n</sub>**) increased, while one of the two bands



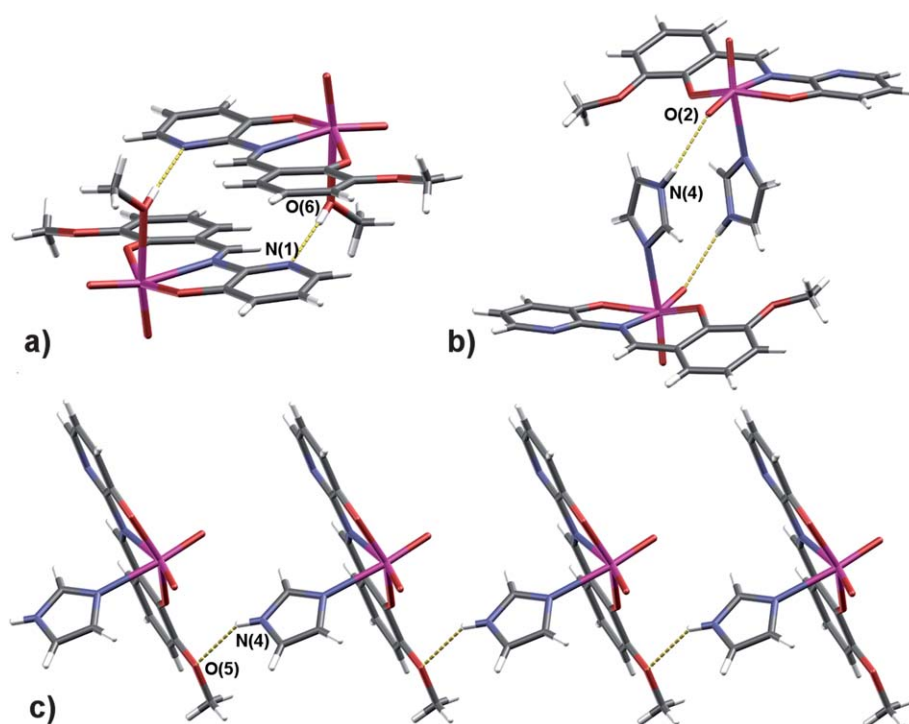


**Fig. 3** Three typical synthons accomplished in the structure of the investigated  $[\text{MoO}_2\text{L}(\text{D})]$  complexes, when an additional hydrogen bond donating group is present in the ancillary ligand (a)  $R_2^2(12)$   $\text{O}(6)\text{--H}(6)\cdots\text{N}(1)$  dimer in alcohol complexes, (b)  $R_2^2(12)$   $\text{N}(4)\text{--H}(4\text{N})\cdots\text{O}(2)$  dimer in the structure of **I(Me)** and (c)  $C_1^1(9)$  chains in the **I(Me)**· $\text{CH}_3\text{CN}$ . Key interaction parameters for **I(Me)**:  $\text{O}(6)\text{--H}(6)\cdots\text{N}(1)$  [ $\text{O}(6)\text{--H}(6)$  0.81(2) Å,  $\text{H}(6)\cdots\text{N}(1)$  1.91(2) Å,  $\text{O}(6)\cdots\text{N}(1)$  2.716(2) Å,  $\text{N1--H1}\cdots\text{O3}$  177(4)°,  $i = 1-x, 1-y, 1-z$ ], **I(Et)**:  $\text{O}(6)\text{--H}(6)\cdots\text{N}(1)$  [ $\text{O}(6)\text{--H}(6)$  0.81(3) Å,  $\text{H}(6)\cdots\text{N}(1)$  1.97(3) Å,  $\text{O}(6)\cdots\text{N}(1)$  2.779(4) Å,  $\text{N1--H1}\cdots\text{O3}$  176(3)°,  $i = -x, 2-y, -z$ ], **I(Pr)**:  $(6)\text{--H}(6)\cdots\text{N}(1)$  [ $\text{O}(6)\text{--H}(6)$  0.77(4) Å,  $\text{H}(6)\cdots\text{N}(1)$  2.01(4) Å,  $\text{O}(6)\cdots\text{N}(1)$  2.760(5) Å,  $\text{N1--H1}\cdots\text{O3}$  167(6)°,  $i = 2-x, -y, -z$ ], **I(Me)**:  $\text{N}(4)\text{--H}(4\text{N})\cdots\text{O}(2)$  [ $\text{N}(4)\text{--H}(4\text{N})$  0.857(2) Å,  $\text{H}(4\text{N})\cdots\text{O}(2)$  2.26(2) Å,  $\text{N}(4)\cdots\text{O}(2)$  2.933(2) Å,  $\text{N}(4)\text{--H}(4\text{N})\cdots\text{O}(2)$  136(2)°, ( $i = -x, 1-y, 1-z$ )] and **I(Me)**· $\text{CH}_3\text{CN}$ :  $\text{N}(4)\text{--H}(4\text{N})\cdots\text{O}(5)$  [ $\text{N}(4)\text{--H}(4\text{N})$  0.83(4) Å,  $\text{H}(4\text{N})\cdots\text{O}(5)$  2.30(4) Å,  $\text{N}(4)\cdots\text{O}(5)$  3.024(5) Å,  $\text{N}(4)\text{--H}(4\text{N})\cdots\text{O}(5)$  146(3)°, ( $i = 1+x, y, z$ ).

characteristic of the  $\text{Mo}=\text{O}_{\text{terminal}}$  vibration gradually disappeared.

Moreover, **I** proved to be sensitive to acetonitrile vapour (Fig. 5), where only a brief exposure promoted the formation of  $\text{Mo}=\text{O}\cdots\text{Mo}$  interactions and the formation of  $(\text{I})_n$  (PXRD). On

a macroscopic scale, this transformation was followed by a change of the sample's colour from orange to brown. The  $\text{Mo}=\text{O}\cdots\text{Mo}$  interaction in the  $(\text{I})_n$  is insensitive to thermal treatment, but a reverse reaction to obtain the amorphous **I** is easily accomplished by grinding.

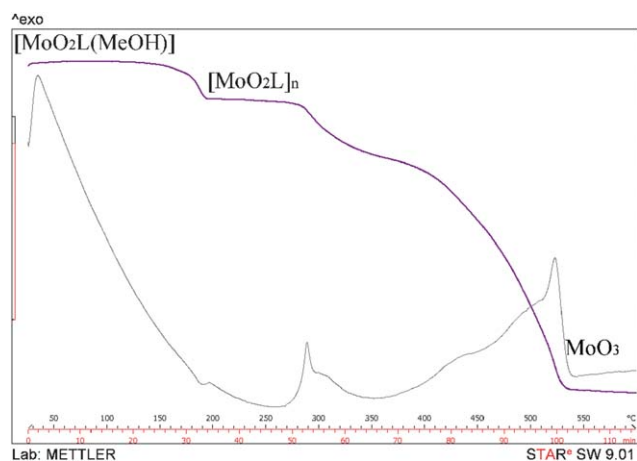


**Fig. 4** Heating of the  $[\text{MoO}_2\text{L}(\text{MeOH})]$  (**I(Me)**) results in the quantitative transformation to the brown  $(\text{I})_n$ , stable in the range of 200–250 °C. Similar curves (with identical products) were obtained for other alcohol complexes **I(Et)** and **I(Pr)**.

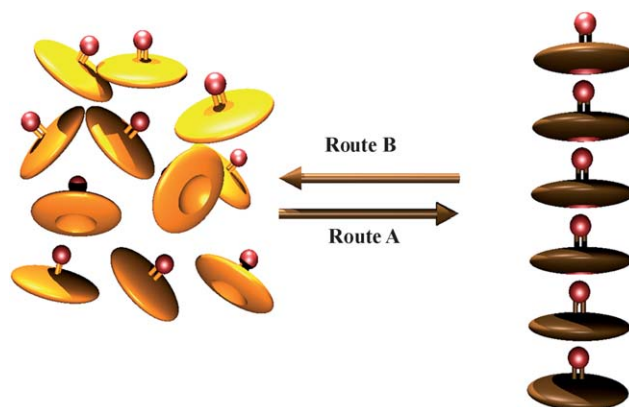


**Fig. 5** Solvent-free routes for interconversion in the **I**/ $(\text{I})_n$  system. Route A: heating to 130 °C or one hour in the acetonitrile vapours (room temperature); Route B: neat grinding (20 min, 25 Hz). **I**—orange;  $(\text{I})_n$ —brown.

Recent studies revealed that mechanochemical manipulation of some metalo-organic compounds with low coordination numbers could lead to remarkable changes in the material's properties, such as its luminescence or colour.<sup>25</sup> These phenomena proved to be unique for each described example.<sup>26,27,28</sup> Mechanochromism and thermochromism in this system arises from the thermally induced formation and mechanochemically induced cleavage of the Mo=O...Mo interaction between the "activated" complex moieties.

Solids that can transfer mechanical force to one distinguished part of the molecule, thus changing their macroscopic physical properties or reactivity, are interesting in the development of stress-sensors and stress-responsive materials.<sup>29</sup>

### Synthesis of [MoO<sub>2</sub>L(D)] complexes from **I** or (**I**)<sub>n</sub>

**I** and (**I**)<sub>n</sub> display similar reactivity towards both O- or N-donating ligands. Both compounds readily coordinate alcohol molecules, even from vapours (ESI, vapour sorption experiments†).

The syntheses of the [MoO<sub>2</sub>L(D)] compounds (D = N-donor), from **I** or (**I**)<sub>n</sub> as precursors, were performed in two ways, by classic solution synthesis and by LAG. Depending upon the solvent used (solution approach), five new products were obtained and structurally characterized, [MoO<sub>2</sub>L(im)] (**I(Im)**), [MoO<sub>2</sub>L(im)]·CH<sub>3</sub>CN (**I(Im)·CH<sub>3</sub>CN**), [MoO<sub>2</sub>L(γ-pic)]·CH<sub>3</sub>CN (**I(Gp)·CH<sub>3</sub>CN**) and the dinuclear complexes [(MoO<sub>2</sub>)<sub>2</sub>(bpy)] (**I(Bp)**) and [(MoO<sub>2</sub>)<sub>2</sub>(bpy)]·CH<sub>2</sub>Cl<sub>2</sub> (**I(Bp)·CH<sub>2</sub>Cl<sub>2</sub>**). In all obtained products, the nitrogen-donating ligand was coordinated to the sixth coordination site.

However, in this particular system, the solution syntheses had a number of disadvantages. Significant amounts of the solvent (dichloromethane and acetonitrile) were needed to dissolve the precursors **I** or (**I**)<sub>n</sub>, while the energy consumption was high due to the prolonged heating, for still relatively low yields. Furthermore, to exclude the possibility of competition between the water and N-donors and to successfully gain target products, the reactions had to be conducted in a dry atmosphere using dry solvents.

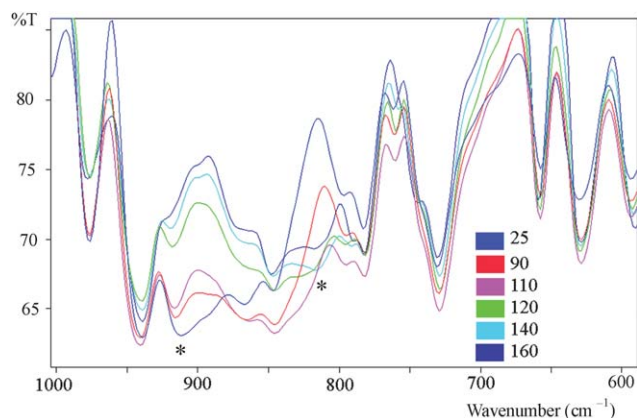


**Fig. 6** Dynamic changes in the TR-IR patterns during the heating of **I**. Bands important for discussion are denoted with an asterisk (diminishing of the Mo=O<sub>term</sub> stretching vibration at 911 cm<sup>-1</sup> and emergence of the Mo=O...Mo band at 814 cm<sup>-1</sup>). Numbers in the right corner correspond to the T/°C at which the spectrum was obtained.

The mechanochemical synthesis of the N-complexes, [MoO<sub>2</sub>L(D)], was attempted by neat grinding with a mortar and pestle, neat grinding in a ball-mill and by LAG using 2–4 drops of acetonitrile or dichloromethane. The neat grinding of **I** or (**I**)<sub>n</sub>, as precursors, with the target N-donor using a mortar and pestle, did not yield the desired compounds, but instead in all cases produced a mixture of **I** and the N-donor. Neat grinding in a ball mill was successful in accomplishing a coordination bond between molybdenum and the N-donor, *i.e.* in yielding the desired products, but they were all amorphous. However, LAG improved the degree of structural order in the collected samples, which were easily distinguished by the PXRD. Grinding in a ball mill jar for 40 min (25 Hz), in the presence of the appropriate solvent, yielded quantitative amounts of the pure products [MoO<sub>2</sub>L(D)] (ESI, Fig. S14†).

In this system, however, the LAG procedure also revealed certain disadvantages. Such an approach was found to be inappropriate for the synthesis of complexes with O-donors (alcohols) and solvates of N-donors (with exception of **I(Gp)·CH<sub>3</sub>CN**). In the case of O-donors, the product collected after LAG was **I**, due to the sensitivity of the Mo–alcohol bonds to mechanical treatment. In the case of N-donors, the unsolvated complexes were obtained (ESI†) in quantitative yields.

### Conclusions

Alcohol molecules in the coordination sphere of octahedral molybdenum(vi) [MoO<sub>2</sub>L(ROH)] complexes provide a good platform for further solid-state manipulations. As a response to stress, induced by mechanical force or heating, such ligands were removed in a selective manner in the solid state, yielding two kinds of coordinatively unsaturated intermediate products, the pentacoordinated amorphous **I** and the polymeric (**I**)<sub>n</sub> of the same composition, [MoO<sub>2</sub>L]. Due to the potential coordination of a solvent molecule or water from solution/atmosphere to the emptied sixth site, no other methods were successful for the synthesis of these intermediates. Both **I** and (**I**)<sub>n</sub> tend to fulfil their coordination spheres and readily coordinate N- and O-donors at the empty coordination site. Noteworthy, [MoO<sub>2</sub>L] precursors could be easily recovered from the emerged six-coordinated species by the above described solvent-free methods.

Although the LAG procedure resulted in improved yields of the target complexes, it proved inferior in the synthesis of the solvated complexes where solvent molecules are weakly bound. Also, due to the cleavage of the molybdenum–alcohol bond, LAG was ineffective in the synthesis of complexes where the coordinated ligands are mechanosensitive. These results proved that both solution and solvent-free methods are superior, one to another, under specific conditions and that their combination is essential for a thorough screening of products and the development of new functional materials. Our future investigations will be concentrated on the study of precursors with two or more mechanosensitive sites and their potential application in the controllable synthesis of higher-ordered coordination networks.

### Acknowledgements

This work was financially supported by the Ministry of Science, Education and Sports of the Republic of Croatia (Grant No.

119-1191342-1082). We are grateful to Dr Ivan Halasz for fruitful discussions.

## References

- 1 (a) S. Kitagawa, R. Kitaura and S.-i. Noro, *Angew. Chem., Int. Ed.*, 2004, **43**, 2334; (b) S. Kitagawa and R. Matsuda, *Coord. Chem. Rev.*, 2007, **251**, 2490.
- 2 (a) P. D. Knight and P. Scott, *Coord. Chem. Rev.*, 2003, **242**, 125; (b) A. K. Cheetham, C. N. R. Rao and R. K. Feller, *Chem. Commun.*, 2006, 4780.
- 3 B. L. Chen, M. Eddaoudi, S. T. Hyde, M. O'Keeffe and O. M. Yaghi, *Science*, 2001, **291**, 1021.
- 4 M. K. Beyer and H. Clausen-Schaumann, *Chem. Rev.*, 2005, **105**, 2921.
- 5 T. Friščić, *J. Mater. Chem.*, 2010, **20**, 7599.
- 6 (a) A. L. Garay, A. Pichon and S. L. James, *Chem. Soc. Rev.*, 2007, **36**, 846; (b) D. Braga, S. L. Giuffreda, F. Grepioni, A. Pettersen, L. Maini, M. Curzi and M. Polito, *Dalton Trans.*, 2006, 1249; (c) D. Braga, S. L. Giuffreda, M. Curzi, Lucia Maini, M. Polito and Fabrizia Grepioni, *J. Therm. Anal. Cal.*, 2007, 90.
- 7 (a) M. Ogawa, T. Hashizume, K. Kuroda and C. Kato, *Inorg. Chem.*, 1991, **30**, 584; (b) N. Shan, F. Toda and W. Jones, *Chem. Commun.*, 2002, 2372; (c) A. Pichon, A. L. Garay and S. L. James, *CrystEngComm*, 2006, **8**, 211.
- 8 G. Kaupp, *CrystEngComm*, 2009, **11**, 388.
- 9 (a) T. Friščić and L. Fábrián, *CrystEngComm*, 2009, **11**, 743; (b) F. C. Stobridge, N. Judaš and T. Friščić, *CrystEngComm*, 2010, **12**, 2409.
- 10 T. Friščić, D. G. Reid, I. Halasz, R. S. Stein, R. E. Dinnebier and M. J. Duer, *Angew. Chem., Int. Ed.*, 2010, **49**, 712.
- 11 (a) D. Braga, S. L. Giuffreda, F. Grepioni and M. Polito, *CrystEngComm*, 2004, **6**, 458; (b) A. V. Trask and W. Jones, *Top. Curr. Chem.*, 2005, **254**, 41.
- 12 (a) R. Kuroda, J. Yoshida, A. Nakamura and S. Nishikiori, *CrystEngComm*, 2009, **11**, 427; (b) C. Bianchini, M. Peruzzini and F. Zanobilli, *Organometallics*, 1991, **10**, 3415; (c) R. Tsuchiya, A. Uehara and E. Kyuno, *Chem. Lett.*, 1974, 21; (d) C. J. Adams, P. C. Crawford, A. G. Orpen, T. J. Podesta and B. Salt, *Chem. Commun.*, 2005, 2457; (e) G. M. Espallargas, L. Brammer, J. v. d. Streek, K. Shankland, A. J. Florence and H. Adams, *J. Am. Chem. Soc.*, 2006, **128**, 9584; (f) N. H. Phan, I. Halasz, I. Opahle, E. Alig, L. Fink, J. W. Bats, P. T. Cong, H.-W. Lerner, B. Sarkar, B. Wolf, H. O. Jeschke, M. l Lang, R. Valentí, R. Dinnebier and M. Wagner, *CrystEngComm*, 2011, **13**, 391–395.
- 13 K. Užarević, M. Rubčić, I. Đilović, Z. Kokan, D. Matković-Čalogović and M. Cindrić, *Cryst. Growth Des.*, 2009, **9**, 5327.
- 14 G. J.-J. Chen, J. W. McDonald and W. E. Newton, *Inorg. Chem.*, 1976, **15**, 2612.
- 15 *Oxford Diffraction*, Oxford Diffraction Ltd., Xcalibur CCD system, CRYCALIS Software system, Version 1.170, 2003.
- 16 G. M. Sheldrick, *SHELXS97, Program for the Solution of Crystal Structures*, University of Göttingen, Germany, 1997.
- 17 G. M. Sheldrick, *Acta Crystallogr., Sect. A: Found. Crystallogr.*, 2008, **64**, 112.
- 18 L. J. Farrugia, *J. Appl. Crystallogr.*, 1999, **32**, 837.
- 19 L. Spek, *J. Appl. Crystallogr.*, 2003, **36**, 7.
- 20 L. J. Farrugia, *J. Appl. Crystallogr.*, 1997, **30**, 565.
- 21 <http://www.povray.org/>.
- 22 C. F. Macrae, P. R. Edgington, P. McCabe, E. Pidcock, G. P. Shields, R. Taylor, M. Towler and J. van de Streek, *J. Appl. Crystallogr.*, 2006, **39**, 453.
- 23 (a) M. Cindrić, N. Strukan, V. Vrdoljak, T. Kajfež and B. Kamenar, *Z. Anorg. Allg. Chem.*, 2002, **628**, 2113; (b) A. Rana, R. Dindo, P. Sengupta, S. Ghosh and L. R. Falvello, *Polyhedron*, 2002, **21**, 1023; (c) M. Cindrić, N. Strukan, T. Kajfež, G. Giester and B. Kamenar, *Z. Anorg. Allg. Chem.*, 2001, **627**, 2604.
- 24 (a) I. Ivanović, K. Andjelković, V. M. Leovac, L. J. Klisarov, M. Lazarević and D. Minić, *J. Therm. Anal.*, 1996, **46**, 1741; (b) O. A. Rajan and A. Chakravorty, *Inorg. Chem.*, 1981, **20**, 660; (c) C. G. Young, Molybdenum. In *Comprehensive Coordination Chemistry*, A. J. McCleverty and T. J. Meyer, ed.; Pergamon, Oxford, 2004, Chapter 4.7, pp 415–527.
- 25 A. L. Balch, *Angew. Chem., Int. Ed.*, 2009, **48**, 2641.
- 26 (a) H. Ito, T. Saito, N. Oshima, N. Kitamura, S. Ishizaka, Y. Hinatsu, M. Wakeshima, M. Kato, K. Tsuge and M. Sawamura, *J. Am. Chem. Soc.*, 2008, **130**, 10044; (b) H. Schmidbaur and A. Schier, *Chem. Soc. Rev.*, 2008, **37**, 1931; (c) A. Y. Lee and R. Eisenberg, *J. Am. Chem. Soc.*, 2003, **125**, 7778.
- 27 T. Abe, T. Itakura, N. Ikeda and K. Shinozaki, *Dalton Trans.*, 2009, 711.
- 28 M. Kojima, H. Taguchi, M. Tsuchimoto and K. Nakajima, *Coord. Chem. Rev.*, 2003, **237**, 183.
- 29 (a) A. L. Black, J. M. Lenhardt and S. L. Craig, *J. Mater. Chem.*, 2011, **21**, 1655–1663; (b) H. Koshima, N. Ojima and H. Uchimoto, *J. Am. Chem. Soc.*, 2009, **131**, 6890.